Amplification and saturation of hot plasma waves driven by runaway electrons in tokamaks

C. Castaldo[1], W. Bin[2], L. Della Volpe[3], F. Napoli[4], P. Buratti[4,5], A. Cardinali[6], M. Guerini Rocco[2], M. Valisa[1], M. Zuin[1], S. Coda[7], J. Decker[7], O. Panico[7], U. Sheikh[7]

[1]*Consorzio RFX, Padova, Italy*

[2]*CNR-ISTP, Milano, Italy*

[3]*Hephaestus Technologies Inc., Camden (Delaware), United States*

[4]*ENEA, NUC Department, Frascati (Roma), Italy*

[5]*INAF-IAPS, Roma, Italy*

[6]*CNR-ISC, Politecnico di Torino, Italy*

[7]*Swiss Plasma Center (SPC) – EPFL, Lausanne, Switzerland*

E-mail: carmine.castaldo@igi.cnr.it

Introduction

Experimental and theoretical studies are extensively pursued, concerning runaway electron (RE) formation in tokamak plasmas and the evolution in time of their distribution function. These studies and their importance for fusion reactors are discussed in [1]. In recent years, the detection of radiofrequency (RF) waves, emitted in the presence of RE in tokamaks [2-5], has opened the search for a new kind of diagnostics. The identification of RF waves driven by RE is indeed a promising method to infer the characteristics of the RE distribution. The wave instabilities can be driven by two RE free energy sources: the anisotropy of the RE distribution, with velocities almost parallel to the magnetic field, and its local peaking in the momentum space, often predicted. Two main interactions occur: the Cherenkov and the anomalous Doppler effects, corresponding respectively to $n = 0$ and $n = -1$ for RE-wave resonances of general form

$$\omega - k_{\parallel} v \mu - n\Omega_{ce}/\gamma = 0. \quad (1)$$

Here $\mu = \cos\theta$, θ is the angle of the electron velocity $\mathbf{v}$ with the static magnetic field $\boldsymbol{B}$, $\Omega_{ce} = -e|\boldsymbol{B}|/m_e c$ and γ is the relativistic factor.

Linear stability analysis of cold plasma waves driven by RE considering any resonance order, with arbitrary RE distribution functions and plasma equilibrium configurations has been discussed in [6]. There, the effective amplification of the unstable waves has been then evaluated by means of a ray-tracing code and based on a statistical analysis of several rays. In [7], the linear stability analysis was performed considering hot plasma waves, by the code REDHPW (**R**unaway **E**lectron **D**riven **H**ot **P**lasma **W**aves). A comparison of the theoretical results with the RF spectra detected in FTU during runaway discharges by ex-vessel antennas suggested that **ion Bernstein waves** (IBW), at their confluence with electron plasma waves (EPW) might be driven unstable by RE, producing characteristics sets of line emissions at frequencies with almost fixed gap of the order of the ion cyclotron frequency f_{ci}. Nonlinear mode coupling seems responsible for the observed line emissions generating frequency gaps of about $f_{ci}/2$. In-vessel antenna in TCV has detected similar sets of line emissions, clearer and better defined.

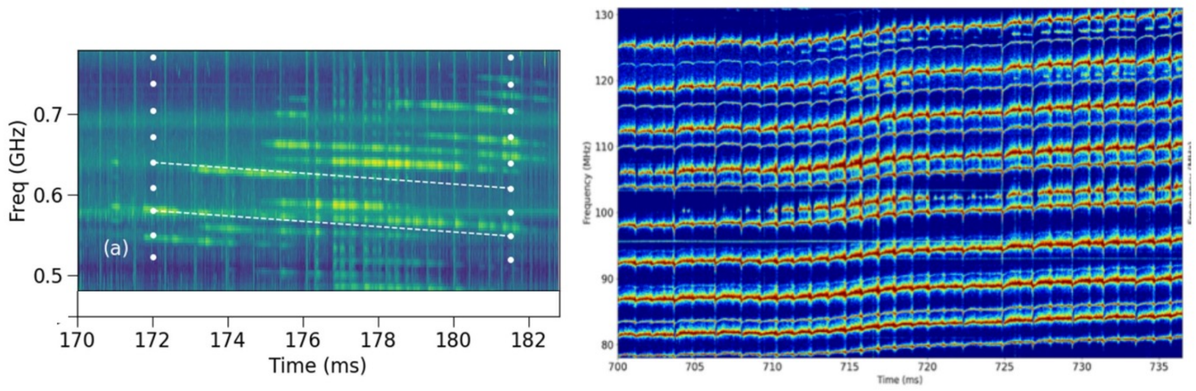

Spectrogram of RF emissions detected in FTU SN 43609 (a). The white circles indicate the frequency of the modes found unstable by REDHPW at the EPW-IBW confluence, where the perpendicular group velocity is zero: the IBW thus propagates along magnetic surfaces, keeping their interaction with RE for sufficient long interval of time to be amplified and detected. Spectrogram of RF emission detected in TCV SN 86969.

Here we evaluate the time evolution and RE-driven amplification of IBW packets emerging from the thermal noise, based on the eikonal theory. The model is implemented by the numerical code **FAREDW** (**F**inite **A**mplitude **R**unaway **E**lectron **D**riven **W**aves). As a reference scenario, we adopt the TCV Deuterium plasma SN 86969 for $t = 0.7$ s and consider the interval of frequency in the range in the frequency range 80-100 MHz, where line emissions at about 87 MHz 93 MHz and 98 MHz were observed. The relevant gap is about $f_{ci}/2$, considering the value of the magnetic field on axis. The frequencies 87 MHz and 98 MHz correspond, respectively to 8 f_{ci} and 9 f_{ci}. We first perform a local linear stability analysis.

Linear stability analysis.

Linear stability analysis of quasi-monochromatic waves is performed considering wave electric fields given by the real part of $\boldsymbol{E}e^{i(\omega t - \boldsymbol{k}\cdot\boldsymbol{r})}$. Here we assume $Re(\omega) = \omega_r > 0$, without any lack of generality. The linear wave equation is

$$\bar{\bar{\Lambda}}\,\boldsymbol{E} = 0, \quad (2)$$

where $\bar{\bar{\Lambda}} = k_\alpha k_\beta c^2 - k^2 c^2 \delta_{\alpha\beta} + \omega^2 \varepsilon_{\alpha\beta}$ is the dispersion tensor in Cartesian components. The dielectric tensor is given by $\bar{\bar{\varepsilon}} = \mathrm{I} + \bar{\bar{\chi}}_{e,M} + \sum_i \bar{\bar{\chi}}_{i,M} + \bar{\bar{\chi}}_{RE}$, $\bar{\bar{\chi}}_{e,M}$ and $\bar{\bar{\chi}}_{i,M}$ are, respectively, susceptibility tensor of the electrons and ions of species i of the plasma background, which is assumed Maxwellian, and provided by analyitic expressions. $\bar{\bar{\chi}}_{RE}$ is the susceptibility tensor of the RE, which is calculated numerically, based on a general relativistic expression, for any given RE distribution function in the momentum space. If both the ordering $|\omega_i| \ll \omega_r$ and $|\varepsilon^A_{\alpha\beta}| \ll |\varepsilon^H_{\alpha\beta}|$ hold, where $\omega_i = Im(\omega)$ and the superscripts A, H denote, respectively, the anti-Hermitian and the Hermitian part, a Taylor expansion provides an approximate solution of the wave equation. We adopt the local Stix reference frame, with Cartesian axis X aligned along the component of the wavenumber perpendicular to the static magnetic field, which is parallel to the axis Z. For any angular frequency ω_r and any parallel refractive index $N_\parallel = k_z c/\omega_r$, normal plasma mode branches are identified, calculating the perpendicular refractive index $N_\perp = k_x c/\omega_r$ as numerical solutions of the dispersion equation

$$\det \bar{\bar{\Lambda}}^H = 0, \quad (3)$$

where $\Lambda^H_{\alpha\beta} = N_\alpha N_\beta - N^2\delta_{\alpha\beta} + \varepsilon^H_{\alpha\beta}$. We neglect the contribution of RE to the Hermitian part of the dielectric tensor ε^H, since their density is much smaller than the plasma density. For each normal plasma mode, the relevant electric field polarization is given by the wave equation

$$\bar{\bar{\Lambda}}^H \boldsymbol{E} = 0 \quad (4)$$

Finally, the imaginary part ω_i is given by

$$\omega_i = i \frac{E^*_\alpha E_\beta \varepsilon^A_{\alpha\beta}}{E^*_\alpha E_\beta \frac{\partial}{\partial\omega_r}\omega_r^2 \varepsilon^H_{\alpha\beta}} \quad (5)$$

2) The anti-Hermitian part of the susceptibility tensor for background electrons and ions due to the collisions, $\bar{\bar{\chi}}^A_{ac}$. The latter is evaluated adopting a simple approximation, i.e. the substitution $\omega \to \omega + i\nu_\alpha$ in the conductivity tensor of the plasma species α: for $\nu_\alpha \ll \omega_r$ one obtains:

$$\bar{\bar{\chi}}^A_{ac} = i\frac{\nu_\alpha}{\omega_r}\left[\bar{\bar{\chi}}^H_{\alpha M}(\omega_r, \boldsymbol{k}) + \omega_r \frac{\partial}{\partial\omega_r}\bar{\bar{\chi}}^H_{\alpha M}(\omega_r, \boldsymbol{k})\right] \quad (7)$$

3) The anti-Hermitian part of the susceptibility tensor of RE, which is calculated numerically, from the integrals of the relativistic expression, for given RE distribution functions. These integrals involve poles corresponding to the resonances (1), which are treated following the Landau prescription. For computational purposes, it is convenient considering the (u, μ) space (the RE distribution are unform in the gyro-angle) where u is the momentum of the electrons normalized to $m_e c$. Owing to the Dirac delta distribution resulting from the Landau prescription to treat the resonance poles, the integrals over μ are calculated analytically, and only 1D numerical integrals over u need to be performed. The plasma parameters on axis for the reference scenario are $B_o = 1.43$ T, $n_{eo} = 1.36\ 10^{13}$ cm^{-3}, $n_{Do} = 7.9\ 10^{12}$ cm^{-3}, $T_{eo} = 1.14$ keV, $T_{io} = 0.5$ keV. Fully ionized ^{12}C is considered as the dominant impurity. Linear profiles of the temperatures and the density vs the normalized poloidal flux ψ_N are assumed, with 30 eV temperature (for both ions and electrons) and 5 10^{11} m^{-3} density at $\psi_N = 1.0$. Since no evidence of significant interaction via anomalous Doppler has been observed around the observation time, it is assumed that the Cherenkov wave-beam interaction is dominant and that the main free energy source is provided by a local peak of the RE distribution function in the momentum space. A skew normal energy distribution and almost gaussian angular distribution is adopted, as already used and described in [11]. In the (E, μ) space this distribution function is given by

$$f(E,\mu) = \frac{n_b}{C\sigma_E}\varphi\left(\frac{E - E_p}{\sigma_E}\right)\Phi\left(\alpha\frac{E - E_p}{\sigma_E}\right)\frac{\exp(\sigma_\theta \mu)}{2\sigma_\theta \sinh\sigma_\theta}. \quad (8)$$

Here C is a normalization constant, such that the integral of f in the (E, μ) space is the beam density n_b. It is assumed $E_p = 7.5$ MeV, $\sigma_E = 4.0$ MeV, $\sigma_\theta = 20$, $\alpha = 1$.

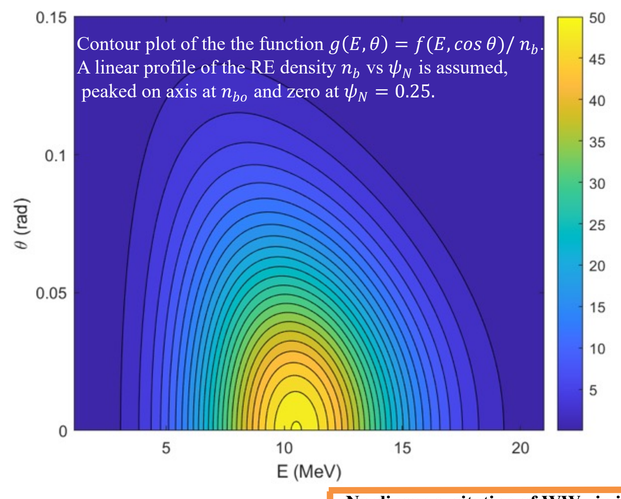

Conclusions

Linear stability analysis suggests that RF line emissions detected by in-vessel antenna in TCV SN 86969 in the range 80-100 MHz might be due to IBW packets originated from the thermal noise and amplified by interaction with RE at the Cherenkov resonance. Line emissions at around 87 MHz and 98 MHz, corresponding to the 8th and 9th harmonics of the deuteron cyclotron frequency are predicted by the modeling and observed in the experiment. Finite amplitude IBW are evaluated, considering the propagation and amplification of wave packets emerging from thermal fluctuations, based on the eikonal theory. Single pass amplification of IBW packet at frequency around 87 MHz is obtained. A saturation level of 60-65 dB above the thermal noise, is reached in a time interval of the order of 10 μs. Further work is necessary to obtain a statistics of IBW packets, in particular concerning their origin in space and detailed frequency spectra should be evaluated. Qusilinear diffusion should be considered to evaluate the evolution of RE distribution function consistently with IBW amplification.

Nonlinear excitation of WW via inverse Landau damping of IBW should be evaluated, possibly explaining the presence of line emissions with half-integer ion cyclotron frequency gaps observed in the spectrograms. An effect of ion heating by collisional and cyclotron damping, suggested by the modeling results as occurring near cyclotron harmonics resonances of IBW with deuterons should be confirmed and compared with experimental observations.

Results of the linear stability analysis.

Linear stability analysis of plasma waves in the presence of RE has been performed considering the plasma parameters on axis of the reference scenario, TCV SN 86969 for $t = 0.7$ s and the RE distribution, skew normal vs. the energy, proposed above, with $n_b = 0.2\ \%\ n_{eo}$. The results are shown in the following plots, as obtained by the numerical coded LeDHPW

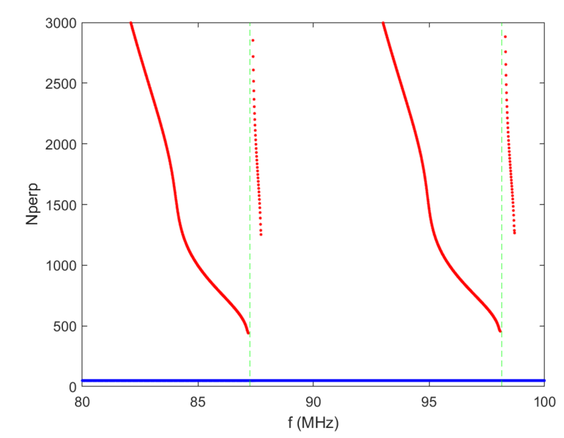

Solution of the dispersion equation for $N_\parallel = 1.0022$, corresponding to the Cherenkov resonance at energy of about 7.2 MeV (where the energy gradient of the RE distribution is positive and near naximum). The IBW branches are shown in red, the whistler wave branch is shown in blue. The vertical, dashed green lines indicate the resonances $f = 8\ f_{cD}$ (~87 MHz) and $f = 9\ f_{cD}$ (~98 MHz)

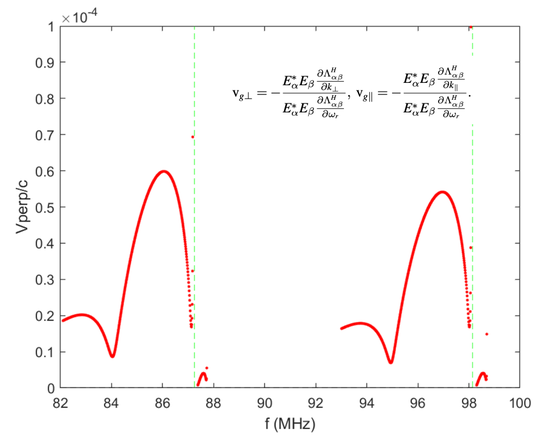

Perpendicular group velocity of IBW waves in units of the speed of light in vacuum. The vertical, dashed green lines indicate the deuteron cyclotron resonances (8th and 9th harmonics). Parallel and perpendicular group velocities are given by the expressions reported in the viewgraph

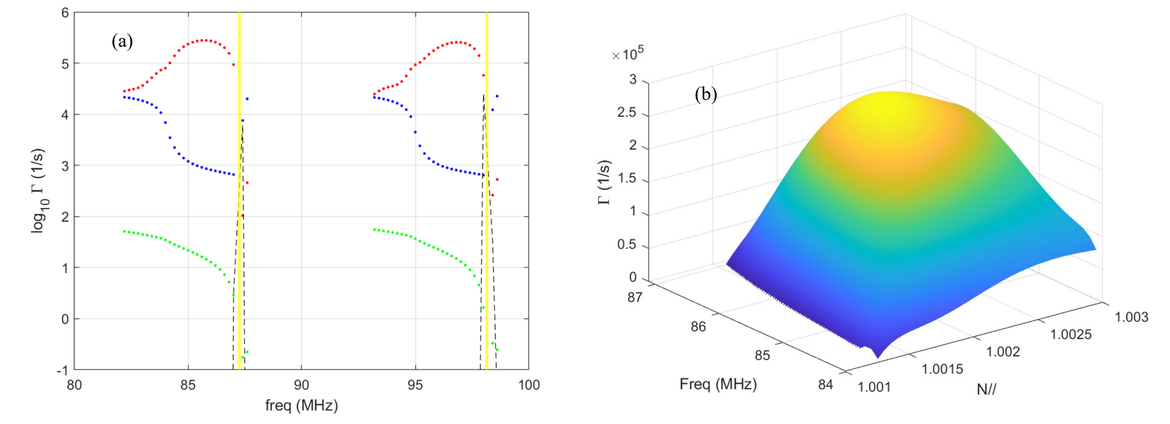

In (a) the growth rate of IBW due to RE drive (red dots), the collisional damping due to ions (blue dots) and electrons (green dots) and the cyclotron damping (dashed lines) vs. the wave frequency, for $N_\parallel = 1.0022$. In (b) and (c) the net growth rates are shown as functions of the parallel refractive index and the wave frequency in the ranges where the IBW are driven unstable by RE within the interval 80-100 MHz considered. We note that, although the calculated WW growth rates are a factor three larger than IBW, almost constant in the overall range 80-100 MHz, the relevant perpendicular group velocity are two orders of magnitude larger, namely about 0.02 c. The ray-tracing analysis indicates that single-pass amplification of WW is negligible compared to IBW, since the WW quickly escape from the region where the RE interaction occurs. Their amplification, as suggested in [6] would require multiple reflection at the edge. The relevant analysis, however, should be performed by full-wave codes, since the eikonal theory is not valid in the region of edge reflections. In addition, wave power transmission to electromagnetic modes propagating towards the wall might introduce significant power losses. Scattering off edge density fluctuations should be also considered.

We also observe that discrete line emissions might be produced by WW, as suggested by full-wave analysis performed in [2], [3], due to power accumulation produced by the finite geometry of the vacuum vessel. However, this effect might result in almost random distribution of the frequency gaps among the line emissions. Conversely, IBW excitation naturally provide almost constant gaps, consistently with the observations. Therefore, we limit the analysis of finite wave energy density evolution to the IBW.

Finite amplitude IBW driven by RE.

The IBW driven unstable by RE are amplificated from the noise level, which can be evaluated from fluctuation-dissipation expression:

$$\frac{dW_{\boldsymbol{k}}}{d^3\boldsymbol{k}} = \frac{k_B T_i}{(2\pi)^3}\frac{\boldsymbol{E}^*_{\boldsymbol{k}}\bar{\bar{\varepsilon}}^A\boldsymbol{E}_{\boldsymbol{k}}}{\boldsymbol{E}^*_{\boldsymbol{k}}\left[\frac{\partial}{\partial\omega}\omega\bar{\bar{\varepsilon}}^H\right]_{\omega=\omega_{\boldsymbol{k}}}\boldsymbol{E}_{\boldsymbol{k}}} \quad (9)$$

Here $dW_{\boldsymbol{k}}/d^3\boldsymbol{k}$ is the spectral density in the wavenumber space of the wave energy per unit of volume. Since the ion Bernstein mode is primarily sustained and damped by the ion response, the effective fluctuation temperature entering the fluctuation–dissipation relation is taken to be T_i. This approximation follows from the dominance of the ion contribution to the dissipative component of the anti-Hermitian dielectric tensor (note that the electron collisional damping is negligible compared to the ion collisional damping). The propagation and amplification (or damping) of IBW packets is evaluated by the eikonal theory. The relevant ray-tracing equations are expressed in cylindrical coordinates r, z, φ with respect to the axis of symmetry of the vacuum vessel as

$$\frac{dr}{dt} = -\frac{\partial H/\partial k_r}{\partial H/\partial\omega}$$

$$\frac{dz}{dt} = -\frac{\partial H/\partial k_z}{\partial H/\partial\omega}$$

$$\frac{dk_r}{dt} = \frac{\partial H/\partial r}{\partial H/\partial\omega}$$

$$\frac{dk_z}{dt} = \frac{\partial H/\partial z}{\partial H/\partial\omega}$$

Here the Hamiltonian H is given by $\det\bar{\bar{\Lambda}}^H$ and ω is the real angular frequency. All the derivatives are calculated analytically. Due to long time required for numerical evolution, the net growth rate for each ray is calculated on appropriate time steps after the ray intagration. The axysimmetry determines for each ray the constant $k_\varphi r$, which is the variable canonically conjugate to the angle φ. The magnetic field and its derivatives are calculated by means of spline interpolations based on the equilibrium reconstruction provided by an EQDSK file. A wave packet, originated from the seed thermal noise at a given point with coordinates r_o, z_o, is defined by a meshgrid in $N_\parallel, f, \eta$, where f is the wave frequency and η is the angle formed by the perpendicular wave number $\boldsymbol{k}_\perp$ with $\boldsymbol{B} \times \nabla\psi_N$: for $\eta = 0$ the perpendicular group velocity is tangent to the magnetic surface in r_o, z_o. The initial conditions for k_r, k_z are obtained by solving the wave dispersion equation with magnetic field and plasma parameters at r_o, z_o: from $N_\parallel$ and f the perpendicular refractive index $N_\perp$ of the IBW branch is determined by numerical solution. Considering the angle η, k_r, k_z and k_φ (hence the constant $k_\varphi r_o$) are then calculated analytically. Finally, the energy density of the wave packet is given at the time step t_n by

$$W(t_n) = \int_{N_{\parallel,1}}^{N_{\parallel,2}} dN_\parallel \int_{f_1}^{f_2} df \int_{\eta_1}^{\eta_2} d\eta \left|\frac{\partial(k_r, k_z, k_\varphi)}{\partial(N_\parallel, f, \eta)}\right|_{t_n} \left\{\left[\frac{dW_{\boldsymbol{k}}}{d^3\boldsymbol{k}}\right]_{t=0}(N_\parallel, f)\right\} \exp 2\int_o^{t_n} dt\, \gamma(t, N_\parallel, f, \eta)$$

The Jacobian, the net growth rate and the above integral are calculated numerically, after mapping all the rays on the same time grid from 0 to t_n

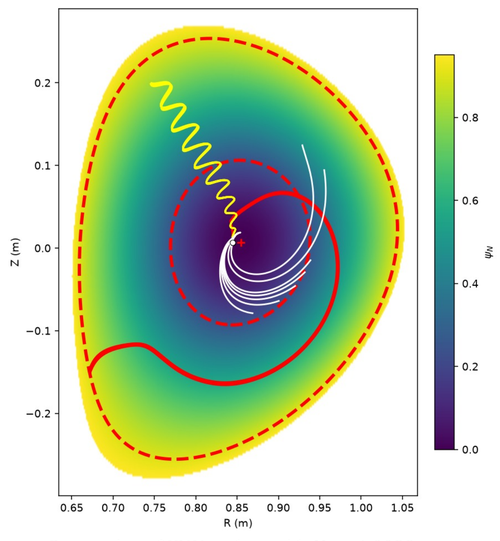

Ray-tracing of IBW packets with $N_\parallel = 1.0022$, η from 0^o to 1.0^o in steps of 0.1^o, for 86.5 MHz (red) 87.0 MHz (yellow) and 87.5 MHz (white). Dashed, red lines correspond to $\psi_N = 0.25$, and $\psi_N = 0.9$. A+, red mark indicates the position of the magnetic axis.

Note that complete IBW absorption is considered for rays crossing deuteron cyclotron harmonics resonances [8]

Finite amplitude IBW driven by RE and emerging from the thermal noise

The amplification and saturation of IBW packets has been evaluated considering 1.0 % n_{eo} peak RE concentration on axis, with distribution $f(E, \mu)$. The RE current is thus 82.5 kA, namely about 38% of the plasma current $I_p = 214$ kA.

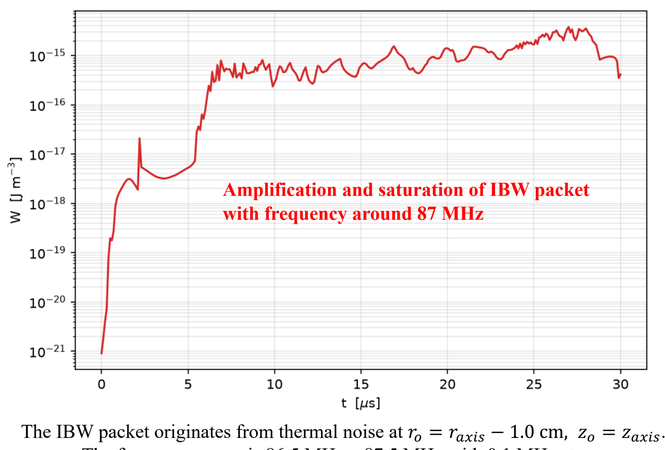

The IBW packet originates from thermal noise at $r_o = r_{axis} - 1.0$ cm, $z_o = z_{axis}$. The frequency range is 86.5 MHz – 87.5 MHz with 0.1 MHz steps, $N_\parallel = 1.0015 - 1.0030$ with 0.0005 steps, η from 0^o to 1.0^o in steps of 0.1^o

References

[1] Breizman B.N., et al. 2019, Nucl. Fusion **59** 083001
[2] Spong D.A. et al 2018, Phys. Rev. Lett. **120** 155002
[3] Heidbrink W.W., et al., 2019, Plasma Phys. Control. Fusion **61** 014007
[4] Buratti P. et al, 2021, Plasma Phys. Control. Fusion **63** 095007
[5] Bin W., et al. 2022, Phys. Rev. Lett. **129** 045002
[6] Aleynikov P. and Breizman B., 2015, Nucl. Fusion **55** 04301
[7] Castaldo C., et al., 2024, Nucl. Fusion **64** 086003
[8] Cardinali A. and Romanelli F., 1992, Phys. Fluids B **4** 511